Controlling Intermolecular Interactions between Metallomesogens: Side-Chain Effects in Discotic Copper, Palladium, and Vanadyl Bis(β-Diketonates)

Hanxing Zheng, Chung K. Lai, and Timothy M. Swager*

Department of Chemistry, University of Pennsylvania, Philadelphia, Pennsylvania 19104-6323

Received June 26, 1995. Revised Manuscript Received August 22, 1995[⊗]

A systematic study of the liquid-crystalline properties of 30 metal bis(β-diketonate) complexes (M = Cu, VO, Pd) that exhibit discotic mesophases is reported. This study has determined that the ability of the metal center to influence the mesophase stability depends upon the density of side chains. In the 10-side-chain complexes series **3**, all of the materials were found to be liquid crystalline. In this series the M = VO analogues were found to have lower melting and clearing points than those with M = Cu and M = Pd. For the 12-side-chain series **4** the opposite is true, and the M = VO materials have substantially higher clearing points. The differences between series **3** and **4** arise from the enhanced core–core interactions that accompany the increased side-chain density. The side-chain-induced organization assists the expression of the metal center's character in determining the stability and nature of the mesophase. The fact that the transition temperatures of the M = Cu and M = Pd compounds differ more in series **4** than in series **3** is also a manifestation of this greater organization. The influence of the metal centers is discussed in the context of intermolecular dative associations and for some phases of the M = VO materials these interactions produce polymeric $(-V{=}O-V{=}O-)_n$ structures.

Introduction

Creating specific molecular superstructures is a universal goal of researchers seeking to develop molecule-based materials with preselected properties. Thermotropic liquid crystals provide a means for assembling superstructures under thermodynamic control; however, the liquid-crystalline state is very delicate, and slight changes in structure can lead to very different phase behaviors.[1] A comprehensive understanding of the thermodynamic factors influencing the stability of one thermotropic liquid-crystalline phase (mesophase) over another must take into account a number of factors. To accomplish structural control, liquid crystal researchers have principally relied on features such as dipolar interactions and molecular shape.[2] However, there is growing interest in the use of designed intermolecular interactions such as charge transfer,[3] hydrogen bonding,[4] and dative bonding[5] to create novel phases and/or increase the range of liquid crystallinity. Liquid crystals incorporating transition metals (metallomesogens) are a growing subclass of mesomorphic substances with unique and potentially useful properties.[6] Central to the understanding of the behavior of metallomesogenic materials, the vast majority of which are unsaturated, is the participation of dative bonding interactions between the metal centers. The inability to precisely understand and control the phase behavior of metallomesogens remains as a formidable obstacle to the utilization of the unique properties displayed by these materials.

We are endeavoring to understand the factors controlling the liquid-crystalline behavior of discotic metal β-diketonate mesogens. Metal β-diketonate complexes are among the best-known classes of coordination compounds, and nearly all of the transition-metal elements display stable complexes of this type. As a result of this chemical diversity these compounds offer many opportunities for the formation of new transition-metal-based materials. Prior investigations of disk-shaped metal bis(β-diketonate)s have focused upon compounds with 4 and 8 side chains (**1** and **2**, respectively).[7] There have also been numerous studies of non-discoid metal diketonate and closely related complexes.[8–11] Despite this intense interest, the current status of liquid crystallinity in discotic metal bis(β-diketonate)s (i.e., **1** and **2**) is limited by high melting points and/or low thermodynamic stability. We recently reported that vanadyl bis(β-diketonate)s, **2** (M = VO), exhibited very limited mesomorphic behavior. However, when the number of

[⊗] Abstract published in *Advance ACS Abstracts,* October 1, 1995.

(1) (a) *Thermotropic Liquid Crystals: Critical Reports on Applied Chemistry*; Gray, G. W., Ed., Society of Chemical Industry: 1987; Vol. 22. (b) Chandrasekhar, S. *Liquid Crystals*, 2nd ed.; Cambridge University Press: Cambridge, 1992.

(2) For a review of the different shapes of liquid crystals see: Demus, D. *Liq. Cryst.* **1989**, *5*, 75.

(3) (a) Green, M. M.; Ringsdorf, H.; Wagner, J.; Wüstefeld, R. *Angew. Chem., Int. Ed. Engl.* **1990**, *29*, 1478. (b) Ringsdorf, H.; Wüstefeld, R.; Zerta, E.; Ebert, M.; Wendorff, J. H. *Angew. Chem., Int. Ed. Engl.* **1989**, *28*, 914.

(4) (a) Kato, T.; Kihara, H.; Kumar, U.; Uryu, T.; Fréchet, J. M. J. *Angew. Chem., Int. Ed. Engl.* **1994**, *33*, 1644. (b) Fouquey, C.; Lehn, J. M.; Levelut, A. M. *Adv. Mater.* **1990**, *5*, 254. (c) Fukumasa, M.; Kato, T.; Uryu, T.; Fréchet, J. M. J. *Chem. Lett.* **1993,** 65. (d) Brienne, M. J.; Gabard, J.; Lehn, J. M.; Stibor, I. *J. Chem. Soc., Chem. Commun.* **1989**, 1868.

(5) (a) Serrette, A. G.; Swager, T. M. *J. Am. Chem. Soc.* **1993**, *115*, 8879. (b) Serrette, A.; Carroll, P. J.; Swager, T. M. *J. Am. Chem. Soc.* **1992**, *114*, 1887. (c) Serrette, A. G.; Swager, T. M. *Angew. Chem., Int. Ed. Engl.* **1994**, *33*, 2342–5.

(6) For reviews on metallomesogens see: (a) Giroud-Godquin, A. M.; Maitlis, P. M. *Angew. Chem., Int. Ed. Engl.* **1991**, *30*, 375. (b) Espinet, P.; Esteruelas, M. A.; Oro, L. A.; Serrano, J. L.; Sola, E. *Coord. Chem. Rev.* **1992**, *117*, 215. (c) Hudson, S. A.; Maitlis, P. M. *Chem. Rev.* **1993**, *93*, 861. (d) Bruce, D. W. In *Inorganic Materials*; Bruce, D. W.; O'Hare, D., Eds.; John Wiley and Sons: New York, 1992; Chapter 8.

0897-4756/95/2807-2067$09.00/0

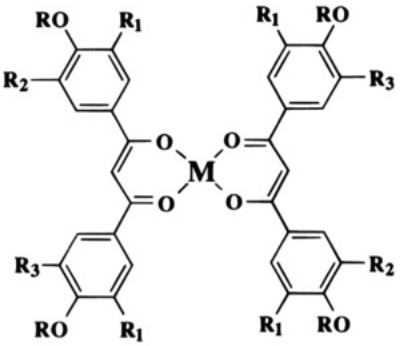

M= Cu, Pd, VO
R= $(CH_2)_nH$
1 $R_1=R_2=R_3=H$
2 $R_1=OR$; $R_2=R_3=H$
3 $R_1=R_2=OR$ $R_3=H$
4 $R_1=R_2=R_3=OR$

side chains in increased to 10 (i.e., **3**, M = VO) the liquid crystalline behavior is greatly improved.[12] Herein we describe a systematic investigation of a series of discotic metal bis(β-diketonate) complexes **3** and **4** (M = Cu, Pd, VO) with greater numbers of side chains (10 and 12) than had been previously investigated. As expected, the nature of the metal center influences the liquid-crystalline behavior. More important is our finding of consistent trends in behavior that show that the influence of the metal on the liquid-crystalline behavior varies widely depending upon the number of side chains. Our studies therefore indicate that an understanding of liquid crystallinity in metallomesogens must consider the interplay of the side-chain density and the accompanying organizational differences, in addition to the nature of the metal center.

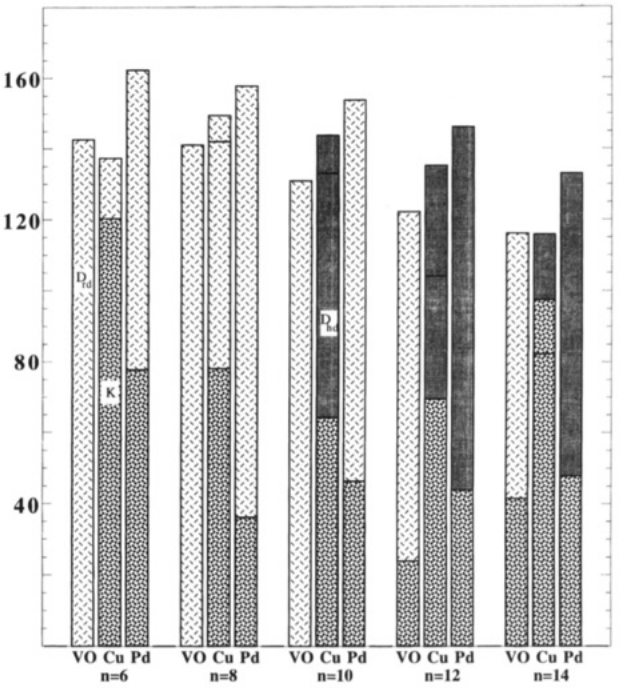

Figure 1. Bar graph showing the phase behavior of discotic compounds of series **3**. Sectors with similar shading have the same phase designation, different metals are indicated under their respective columns, n is the number of carbons in the side chains, K indicates a crystal phase, D_{hd} indicates a hexagonal disordered columnar phase, and D_{rd} indicates a rectangular disordered columnar phase.

Results and Discussion

Synthesis. The β-diketonate ligands were synthesized by straightforward condensation of the appropriate methyl benzoate ester and the acetophenone derivatives as shown in Scheme 1. The 3,4-dialkoxyacetophenone, **5**, is produced by Friedel–Crafts acetylation of the 1,2-dialkoxybenzene. The 3,4,5-trialkoxymethyl benzoate, **6**, is prepared as previously reported.[11d] In addition to serving as an ester for condensation, **6** may also be transformed into the 3,4,5-trialkoxyacetophenone, **7**, by hydrolysis and subsequent reaction with 2 equiv of methyllithium. Reactions of the ligands with $Cu(OAc)_2$, $Pd(OAc)_2$, and $VO(SO_4)$ produced the bis(β-diketonates) in high yields. Satisfactory analyses for all compounds were obtained after several careful recrystallizations (precipitations) and are given in the Experimental Section.

Complexes with 10 Side Chains. The 10 side-chain series, **3**, all display thermodynamically stable (enantiotropic) mesophases as shown in Figure 1. Increasing the side-chain length has the effect of lowering the clearing points, whereas the melting points initially decrease and then increase with a lengthening of the side chains. As is often the case in metallomesogens, the metal complexes are coordinately unsaturated and are capable of exhibiting intermolecular dative interactions.[6] Dative interactions are of particular interest for the square pyramid vanadyl complexes since they produce linear chain structures (e.g., $(-V{=}O-V{=}O-)_n$) and can thereby result in polar order

(7) (a) Giroud-Godquin, A. M.; Gauthier, M. M. *Mol. Cryst. Liq. Cryst.* **1986**, *132*, 35. (b) Ohta, K.; Muroki, H.; Takagi, A.; Yamamoto, I.; Matszaki, K. *Mol. Cryst. Liq. Cryst.* **1986**, *135*, 247. (c) Ohta, K.; Ema, H.; Muroki, H.; Yamamoto, I.; Matsuzaki, K. *Mol. Cryst. Liq. Cryst.* **1987**, *147*, 61. (d) Sakashita, H.; Nishitani, A.; Sumiya, Y.; Terauchi, H.; Ohta, K.; Yamamoto, I. *Mol. Cryst. Liq. Cryst.* **1988**, *163*, 211. (e) Prasad, V.; Sadashiva, B. K. *Mol. Cryst. Liq. Cryst.* **1991**, *195*, 161. (f) Poelsma, S. N.; Servante, A. H.; Fanizzi, F. P.; Maitlis, P. M. *Liq. Cryst.* **1994**, *16*, 675. (g) Godqui-Giroud, A. M., Sigaud, G., Achard, M. F., Hardouin, F. *J. Phys. Lett.* **1984**, *45*, L387. (h) Ohta, K.; Ema, H.; Muroki, H.; Yamamoto, I.; Matsuzaki, K. *Mol. Cryt. Liq. Cryst.* **1987**, *147*, 61. (i) Styring, P.; Tantrawong, S.; Beattie, D. R.; Goodby, J. W. *Liq. Cryst.* **1991**, *10*, 581. (j) Tantrawong, S.; Styring, P.; Goodby, J. W. *J. Mater. Chem.* **1993**, *3*, 1209.

(8) For reports of diketonate based mesogens that exhibit nematic or smectic liquid crystallinity see: (a) Chandrasekhar, S.; Raja, V. N.; Sadashiva, B. K. *Mol. Cryst. Liq. Cryst.* **1988**, *163*, 211. (b) Ohta, K.; Takenata, O.; Hasebe, H.; Morizumi, Y.; Fujimoto, T.; Yamamoto, I. *Mol. Cryst. Liq. Cryst.* **1991**, *195*, 103. (c) Baena, M. J.; Espinet, P.; Ros, M. B.; Serrano, J. L. *Angew. Chem., Int. Ed. Engl.* **1991**, *30*, 711. (d) Sadashiva, B. K.; Ghode, A.; Rao, P. R. *Mol. Cryst. Liq. Cryst.* **1991**, *200*, 187. (e) Baena, M. J.; Espinet, P.; Ros, M. B.; Serrano, J. L.; Ezcurra, A. *Angew. Chem., Int. Ed. Engl.* **1993**, *32*, 1203. (f) Rourke, J. P.; Fanizzi, F. P.; Salt, N. J. S.; Bruce, D. W.; Dunmur, D. A.; Maitlis, P. M. *J. Chem. Soc., Chem. Commun.* **1990**, *229*. (g) Thompson, N. J.; Gray, G. W.; Goodby, J. W.; Toyne, K. J. *Mol. Cryst. Liq. Cryst.* **1991**, *200*, 109.

(9) For nondiscoid β-diketonate complexes that display columnar phases see: (a) Barberá, J.; Cativiela, C.; Serrano, J. L.; Zurbano, M. M. *Adv. Mater.* **1991**, *3*, 602. (c) Atencio, R.; Barberá, J.; Cativiela, C.; Lahoz, F. J.; Serrano, J. L.; Zurbano, *J. Am. Chem. Soc.* **1994**, *116*, 11558. (d) Ohta, K.; Takenata, O.; Hasebe, H.; Morizumi, Y.; Fujimoto, T.; Yamamoto, I. *Mol. Cryst. Liq. Cryst.* **1991**, *195*, 135. (e) Ohta, K.; Morizumi, Y.; Akimoto, H.; Takenata, O.; Fujimoto, T.; Yamamoto, I. *Mol. Cryst. Liq. Cryst.* **1992**, *214*, 143.

(10) For reports of mesomorphic octahedral β-diketonate complexes see: (a) Zheng, H.; Swager, T. M. *J. Am. Chem. Soc.* **1994**, *116*, 761. (b) Giroud-Godquin, A.-M.; Rassat, A. *C. R. Acad. Sc. Paris, Ser. II.* **1992**, *294*, 241.

(11) Related polyketonate derived liquid crystals have also been reported: (a) Barberá, J.; Giménez, R.; Serrano, J. L. *Adv. Mater.* **1994**, *6*, 470. (b) Lai, C. K.; Serrette, A. G.; Swager, T. M. *J. Am. Chem. Soc.* **1992**, 114, 7949. (c) Zheng, H.; Lai, C. K.; Swager, T. M. *Chem. Mater.* **1994**, *6*, 101. (d) Serrette, A. G.; Lai, C. K.; Swager, T. M. *Chem. Mater.* **1994**, *6*, 2252.

(12) Zheng, H.; Carroll, P. J.; Swager, T. M. *Liq. Cryst.* **1993**, *14*, 1421.

Scheme 1[a,b]

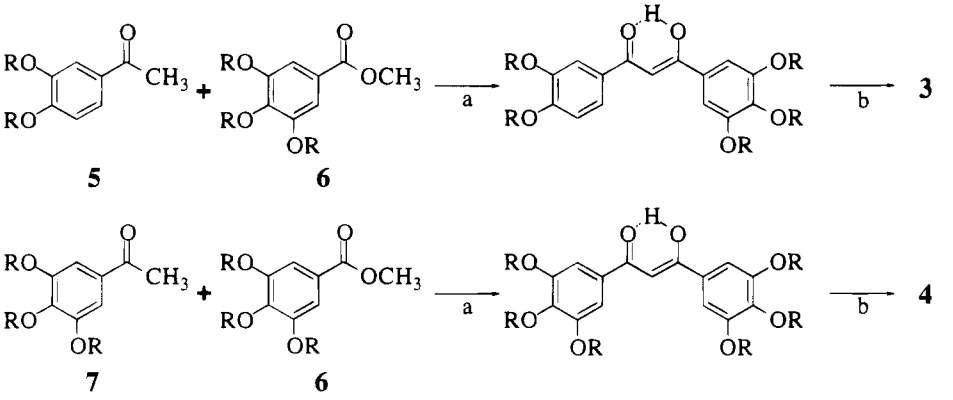

[a] NaH, dimethoxyethane. [b] $Cu(OAc)_2$ or $Pd(OAc)_2$ or $VO(SO_4)$.

along the column axis.[5] This type of polar order is attractive since it offers new possibilities for the generation of novel ferroelectric/piezoelectric and NLO materials.[5,13]

The identification of the discotic phases was performed by observation of the optical textures with a polarizing microscope (Figure 2) and by variable-temperature X-ray diffraction (XRD, (Table 1).[14] Many of the rectangular phases are easily recognized by their mosaic textures which display prominent wedge-shaped defect patterns (Figure 2, plate 1). As shown in plate 6, Figure 2, well-developed spiral domains can sometimes be produced, and for the D_{rd} phases the extinction brushes do not align with the polarizers. In spiral domains the columns are approximately parallel to the glass slides, and hence this feature indicates that the mesogens are tilted with respect to the column normal.[15] In D_{rd} phases with $C(2/m)$ symmetry, the tilt angle can be determined directly from these patterns.[11d,15] The hexagonal phases (D_{hd}) generally display fan textures (Figure 2, plate 2), linear birefringent defects, and large areas of uniform extinction (Figure 2, plate 5). For compounds displaying multiple D_{hd} phases, cooling into the lower temperature D_{hd} phase can transform the fans into highly colored fingerprint textures as shown for **3** (M = Cu, n = 10) in Figure 2, plates 2–4. In other cases, $D_{hd} \rightarrow D_{hd}$ transitions were observed to produce fine disclination lines (needles) throughout the fans (Figure 2, plate 5).[16] Note that the intersections of the needles are related to the hexagonal superstructure and occur at 90° and 30°.

Table 1. Variable-Temperature XRD Data for the Liquid-Crystal Phases of Series 3

compound	mesophase	lattice constant (Å)	spacing (Å) obsd (calcd)	Miller indexes
3, M = Cu				
n = 6	D_{rd}, $P_{(2/a)}$ at 100 °C	a = 50.74	25.37 (25.37)	(200)
		b = 26.54	23.52 (23.52)	(110)
			8.9 (8.85)	(030)
n = 8	D_{rd}, $P_{(21/a)}$ at 143 °C	a = 43.36	23.42	(110)
		b = 27.83	21.68	(200)
	D_{rd}, $P_{(21/a)}$ at 109 °C	a = 43.36	23.61 (23.61)	(110)
		b = 28.15	21.68 (21.68)	(200)
			12.78 (12.86)	(310)
n = 10	D_{hd} at 131 °C	a = 28.30	24.51 (24.51)	(100)
			14.35 (14.15)	(110)
	D_{hd} at 100 °C	a = 28.91	25.04 (25.04)	(100)
			14.28 (14.46)	(110)
n = 12	D_{hd} at 118 °C	a = 30.91	26.77 (26.77)	(100)
			15.54 (15.46)	(110)
			13.39 (13.39)	(200)
	D_{hd}at 74 °C	a = 31.94	27.66 (27.66)	(100)
			15.97 (15.97)	(110)
n = 14	D_{hd} at 100 °C	a = 34.57	29.94 (29.94)	(100)
			17.40 (17.29)	(110)
			14.90 (14.97)	(200)
3, M = Pd				
n = 6	D_{rd}, $P_{(21/a)}$ at 126 °C	a = 37.74	21.20	(110)
		b = 25.63	18.87	(200)
n = 8	D_{rd}, $P_{(21/a)}$ at 118 °C	a = 42.56	23.14 (23.14)	(110)
		b = 27.57	21.28 (21.28)	(200)
			12.61 (12.61)	(310)
n = 10	D_{rd}, $P_{(21/a)}$ at 90 °C	a = 48.56	26.10 (26.10)	(110)
		b = 30.95	24.28 (24.28)	(200)
			14.26 (14.34)	(310)
n = 12	D_{hd} at 137 °C	a = 30.48	26.40	(100)
	D_{hd} at 118 °C	a = 30.76	26.64 (26.64)	(100)
			15.46 (15.38)	(110)
			13.33 (13.32)	(200)
n = 14	D_{hd} at 114 °C	a =32.87	28.47 (28.47)	(100)
			16.60 (16.44)	(110)
			14.25 (14.24)	(200)
	D_{hd} at 83 °C	a = 33.53	29.04 (29.04)	(100)
			16.80 (16.77)	(110)
			14.53 (14.52)	(200)
3, M = VO				
n = 6	D_{rd}, $C_{(2/m)}$ at 118 °C	a = 44.68	22.34 (22.34)	(110)
		b = 17.77	16.51 (16.51)	(200)
			11.49 (11.41)	(310)
n = 8	D_{rd}, $P_{(21/a)}$ at 118 °C	a = 38.22	22.34 (22.34)	(110)
		b = 27.53	19.11 (19.11)	(200)
			11.63 (11.56)	(310)
n = 10	D_{rd}, $P_{(21/a)}$ at 100 °C	a = 43.04	24.41 (24.41)	(110)
		b = 29.64	21.52 (21.52)	(200)
			12.98 (12.91)	(310)
n = 12	D_{rd}, $P_{(21/a)}$ at 100 °C	a = 47.22	26.40 (26.40)	(110)
		b = 31.84	23.61 (23.61)	(200)
			14.18 (14.18)	(310)
n = 14	D_{rd}, $P_{(21/a)}$ at 96 °C	a = 52.33	27.66 (27.66)	(110)
		b = 32.58	26.16 (26.16)	(200)
			15.38 (15.38)	(310)

(13) This type of organization is thought to also be present in bowlic liquid crystals. (a) Lei, L. *Mol. Cryst. Liq. Cryst.* **1987**, *146*, 41 and reference therein. (b) Poupko, R.; Luz, Z.; Spielberg, N.; Zimmermann, H. *J. Am. Chem. Soc.* **1989**, *111*, 6094. (c) Kranig, W.; Spiess, H. W.; Zimmermann, H. *Liq. Cryst.* **1990**, *7*, 123. (d) Levelut, A. M.; Malthete, J.; Collet, A. *J. Phys. (Paris)* **1986**, *47*, 351. (e) Cometti, G.; Dalcanale, E.; Du vosel, A.; Levelut, A. M. *J. Chem. Soc., Chem. Commun.* **1990**, 163. (f) Wang, L.; Sun, Z.; Pei, X.; Zhu, Y. *Chem. Phys.* **1990**, *142*, 335. (g) Malthete, J. *Adv. Mater.* **1994**, *6*, 315 and references therein. (g) Komori, T; Shinkai, S. *Chem. Lett.* **1993**, 1455. (h) Zimmerman, H.; Poupko, R.; Luz, Z.; Billard, J. *Z. Naturforsch., A: Phys., Phys. Chem. Kosmophys.* **1985**, *40A*, 149. (i) Xu, B., Swager, T. M. *J. Am. Chem. Soc.* **1993**, *115*, 1159. (j) Xu, B.; Swager, T. M. *J. Am. Chem. Soc.* **1995**, *117*, 5011. (k) Swager, T. M.; Xu, B. *J. Inclus. Phenom.* **1995**, *18*, 1.

(14) For reviews on discotics see: (a) Destrade, C.; Foucher, P.; Gasparoux, H.; Nguyen H. T.; Levelut, A. M.; Malthete, J. *Mol. Cryst. Liq. Cryst.* **1984**, *106*, 121. (b) Billard, J. In *Liquid Crystals of One- and Two-Dimensional Order*; Springer Series in Chemical Physics; Springer-Verlag: Berlin, 1980; p 383. (c) Chandrasekhar, S.; Ranganath, G. S. *Rep. Prog. Phys.* **1990**, *53*, 57 and references therein.

(15) (a) Chandrasekhar, S. In *Advances in Liquid Crystals*; Brown, G. H., Ed.; Academic Press: New York, 1982; Vol. 5, p 47. (b) Frank, F. C.; Chandrasekhar, S. *J. Phys.* **1980**, *41*, 1285.

(16) Needle patterns have been observed previously. Destrade, C.; Gasparoux, H.; Babeau, A.; Tinh, N. H.; Malthete, J. *Mol. Cryst. Liq. Cryst.* **1981**, *67*, 37.

Plate 1

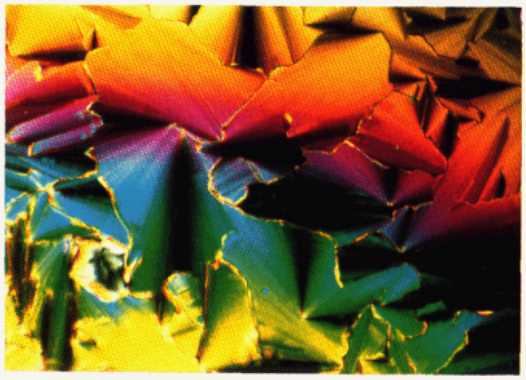

Plate 2

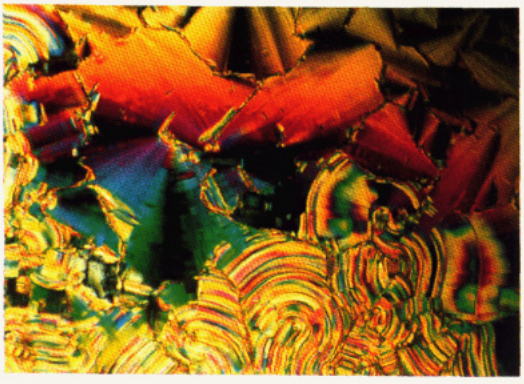

Plate 3

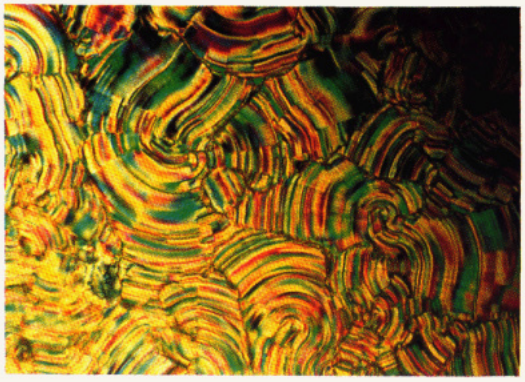

Plate 4

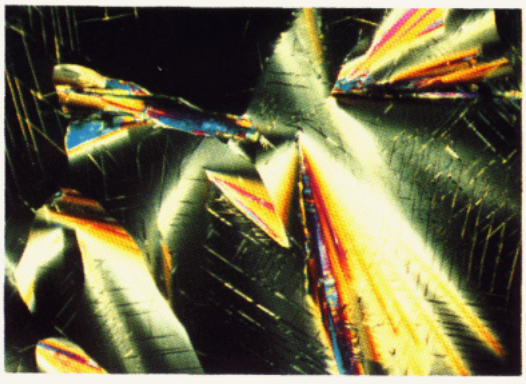

Plate 5

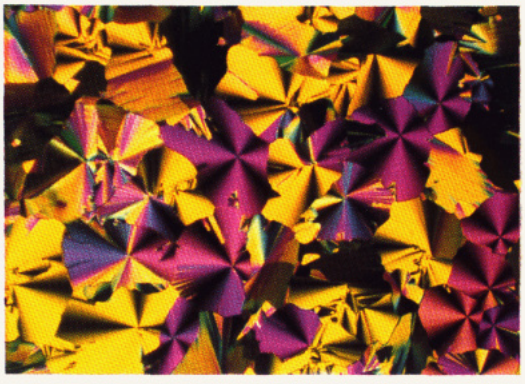

Plate 6

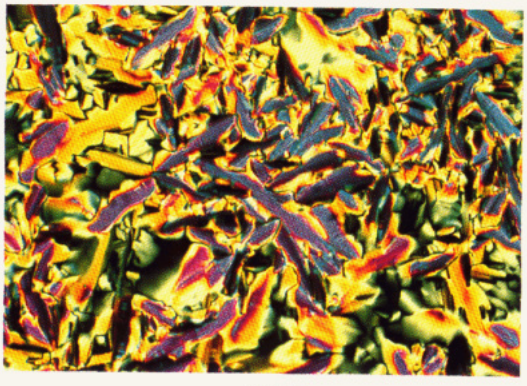

Plate 7

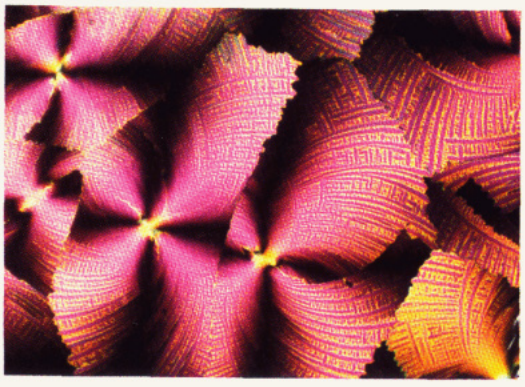

Plate 8

Figure 2. Optical textures of discotic metal bis(β-diketonates) taken with the polarizers in a vertical and horizontal orientation. Plate 1: Mosaic texture of the D_{rd} phase of **3** (M = Cu, n = 8) at 148 °C. Plates 2–4: Sequential photographs of the same region of **3** (M = Cu, n = 10) at 140 °C undergoing a $D_{hd} \rightarrow D_{hd}$ phase transition. Plate 5: Texture of the lower temperature D_{hd} phase of **3** (M = Cu, n = 10) at 134 °C, showing large homeotropic regions of uniform extinction retained from the high-temperature D_{hd} phase and needle features that appear upon entering the low-temperature D_{hd} phase. Plate 6: Texture of the D_{rd} phase of **3** (M = VO, n = 8) at 130 °C. The spiral structures are violet in color and have well-defined extinction brushes that are not aligned with the polarizers. Plate 7: Spine texture of the D_{hd} phase of **4** (M = Pd, n = 14) at 96 °C. Plate 8: Feather texture of the D_{rd} phase of **4** (M = Cu, n = 6) at 110 °C.

Table 2. DSC (10 °C/min) Data for Series 3 (Transition Temperatures (°C) and Enthalpies (in Parentheses, kcal/mol) for Heating and Cooling Cycles Given Above and Below the Arrows, Respectively

Cu	$n = 6$	K	120.3 (10.5) / 80.4 (4.54)	D_{rd}	137.4 (0.61) / 132.0 (0.55)	I		
	$n = 8$	K	78.1 (18.2) →	D_{rd}	142 (<0.01) / 138 (<0.01)	D_{rd}	149.4 (2.38) / 147 (2.31)	I
	$n = 10$	K	64.1 (22.7) →	D_{hd}	133.0 (0.02) / 130.6 (0.01)	D_{hd}	143.8 (2.31) / 140.5 (2.25)	I
	$n = 12$	K	69.4 (35.0) →	D_{hd}	104 (<0.01) / 103 (<0.01)	D_{hd}	135.2 (2.29) / 132.3 (2.69)	I
	$n = 14$	K	82.2 (14.0) →	K	97.5 (27.4) →	D_{hd}	115.8 (1.35) / 110.4 (1.03)	I
			← 63.4 (41.2)					
Pd	$n = 6$	K	77.7 (11.6) →	D_{rd}	162.3 (1.47) / 155.4 (1.13)	I		
	$n = 8$	K	36.2 (1.85) →	D_{rd}	157.7 (1.27) / 150.1 (2.33)	I		
	$n = 10$	K	46.4 (7.61) / 31.7 (4.75)	D_{rd}	153.7 (1.71) / 148.5 (1.81)	I		
	$n = 12$	K	32.0 (4.3) / 24.8 (4)	K	43.9 (6.13) / 32.2 (6)	D_{hd}	134 (<0.01) / 131 (<0.01)	D_{hd} 146.1 (2.27) / 142.2 (2.16) I
	$n = 14$	K	47.9 (18.0) / 36.5 (19.9)	D_{hd}	96 (<0.01) / 92 (<0.01)	D_{hd}	133.0 (0.66) / 129.2 (1.53)	I
VO	$n = 6$	D_{rd}	142.6 (2.34) / 136.0 (2.19)	I				
	$n = 8$	D_{rd}	141.1 (2.28) / 134.9 (2.11)	I				
	$n = 10$	D_{rd}	130.9 (2.09) / 126.9 (1.98)	I				
	$n = 12$	K	23.9 (19.9) / 14.4 (19.9)	D_{rd}	122.2 (2.11) / 119.4 (2.06)	I		
	$n = 14$	K	41.5 (31.6) / 31.1 (31.7)	D_{rd}	116.1 (1.54) / 112.1 (1.65)	I		

All of the materials were investigated by XRD. In these measurements the liquidlike correlations within the columns preclude distinct peaks at wide angle, and in general only broad halos are observed. Hence the phases can be labeled as D_{hd} and D_{rd}, and the "d" subscript indicates a disordered liquidlike organization of mesogens in the columns.[14] Consistent with the characterization of the phases as disordered, the DSC data (Table 2) shows the clearing enthalpies to be very small, thereby indicating a high-entropy mesophase. The transition temperatures given in Table 2 are the peak maximums and indicate that the mesophases are prone to only very minor supercooling. The D_{hd} phases are readily identified by XRD and display a dominant (100) reflection which is often accompanied by low-intensity (110) and (200) peaks. Rectangular columnar phases generally display two intense low angle peaks which index to (110) and (200) reflections, and these phases can exhibit $C(2/m)$, $P(2/a)$, and $P(2_1/a)$ symmetry as shown in Figure 3.[14] The symmetries cannot be determined by optical textures, and assignment requires the use of systematic absences in the XRD and consideration of the lattice dimensions in relation to the molecular dimensions. Materials displaying a (030) reflection are excluded from $C(2/m)$ and $P(2_1/a)$ which do not allow odd $0k$ reflections.[17] Hence a rectangular phase with a peak indexing to (030) must have $P(2/a)$ symmetry. As can be seen from Figure 3, the $C(2/m)$ phase produces a greater difference between the lattice parameters **a** and **b**. We used this fact to determine the difference between $C(2/m)$ and $P(2_1/a)$.

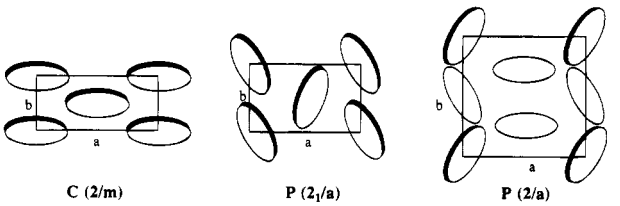

Figure 3. Symmetries and unit cells of the two-dimensional rectangular lattices observed for D_{rd} phases. The dark edges of the disks indicate that the molecules are tilted out of the plane of the paper.

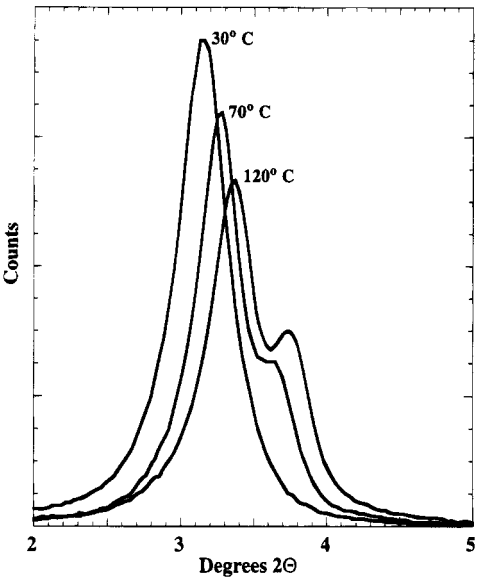

Figure 4. Low-angle XRD data for **3** (M = VO, $n = 12$) which shows a merging of the (200) and (110) diffraction peaks at low temperature.

It is common to see a temperature dependence of the lattice parameters in liquid crystals, and we find that the low-angle reflections of **3** generally shift to larger d spacing with decreasing temperature, indicating a lattice expansion. For the D_{rd} phases of **3** M = VO with $n = 12$, 14, we have found that the (110)/(200) splitting has a marked temperature dependence, indicating an anisotropic contraction of the 2D rectangular lattice in addition to shifting to larger d spacing. As shown in Figure 4, at high temperature the two peaks are clearly evident, but at room temperature they are coincident. Hence at room temperature the phase is indistinguishable from a D_{hd} material at the resolution of our diffractometer. We note this behavior in particular because our initial investigations of **3** (M = VO, $n = 12$) were limited to diffraction experiments at room temperature.[12] This structural change occurs over a very large temperature region and no DSC or textural changes are apparent. Hence it appears that the D_{rd} phase slowly transforms to a D_{hd} structure. This behavior is interesting in the context of what is known about the D_{hd} to D_{rd} transition. High-resolution XRD studies of monodomains have determined that D_{hd}

(17) *International Tables for X-Ray Crystallography*; The Kynoch Press: Birmingham, U.K., 1969; Vol. I, Table 4.2.

phases have finite tilt, and these phases interconvert by a first-order transition involving an orientational ordering–disordering of tilt direction.[18]

The nature of a mesophase and the range of its mesomorphism are determined by both the side-chain length and the transition metal center. For **3** (M = Cu and M = Pd) we observe a transition from discotic rectangular phases (D_{rd}) to discotic hexagonal phases (D_{hd}) with increased side-chain length. We have previously observed a similar D_{rd} to D_{hd} crossover in related bimetallic complexes, and in general we believe that the shorter side-chain complexes favor greater core interactions afforded by the D_{rd} phase.[12d] The tilted D_{rd} phase reduces the interactions between the bulky side chains and allows closer contacts between cores. Additional dative interactions are facilitated by offset between the cores in a D_{rd} phase which allows the Cu and Pd centers to coordinate the oxygen atoms of a neighboring β-diketonate ligands in their axial positions. The greater dispersion forces commensurate with an increase in side-chain length results in a transition to the D_{hd} phase with reduced core–core interactions.

Consistent with our previous studies on discotic antiphases, we find that the M = Pd analogues exhibit higher clearing points than the copper derivatives.[11c] This suggests that the Pd centers produce greater interactions between the core groups which may be the result of dipolar or intermolecular dative interactions. Consistent with increased core interactions, we find that the D_{rd} to D_{hd} changeover for the M = Pd analogue occurs with longer side chains (D_{hd} when $n \geq 12$) relative to the M = Cu complex which displays a D_{hd} phase with $n \geq 10$. Hence for the Pd complexes a larger dispersive force is necessary to stabilize the D_{hd} phase.

The M = VO analogues with their square pyramid structures are conspicuously different than the M = Cu and M = Pd materials, and these complexes display D_{rd} phases irrespective of the side-chain length. In all cases within series **3**, the vanadyl complexes exhibit lower melting and clearing temperatures than the respective M = Cu and M = Pd materials. The lower transition temperatures reflect weakened intermolecular forces resulting from the nonplanar nature of the VO center and/or disorder emanating from a random orientation of the V=O dipoles. As mentioned earlier, there is the interesting possibility of a weak polymeric association (e.g., $(-V{=}O{-}V{=}O{-})_n$) in the mesophase. A V=O stretching band at 898 cm^{-1} (^{18}O 860 cm^{-1}, calcd 859 cm^{-1}) and a yellow color indicate that samples recrystallized from CH_2Cl_2/EtOAc display a polymeric structure.[5] In the isotropic phase the complexes turn light green, and a V=O stretching frequency of 992 cm^{-1} is observed which is consistent with a monomeric structure. Cooling the isotropic phase into the mesophase produces a slight shift of the V=O stretching band to 985 cm^{-1}. For compounds **3** (M = VO, n = 12, 14), which display a D_{rd} to crystal transition, a shift in the V=O stretching band to 898 cm^{-1} accompanies the transformation to the crystal phase. This indicates that any polymeric association in the liquid-crystalline phases of the present compounds must be very weak, and in the limiting case the intermolecular interactions may be best considered to be purely dipolar. Nevertheless, a strong polymeric association is reestablished for **3** (M = VO, n = 12, 14) in the crystal phase.

The reason for the dominance of D_{rd} phases in the M = VO materials is unclear. We suspect that the differences are attributed to the organizational preferences of the polar V=O group. At first glance, we expected that the linear chain structure would favor a D_{hd} phase since the V=O bond is best described as a triple bond which should prefer a linear V=O–V arrangement. This is however inconsistent with the D_{rd} phases which were observed to be tilted (Figure 2, plate 6). It has been reported in other discotic liquid crystals with dipoles normal to the disk plane that the dipoles arrange so as to form antiparallel dimers with a slight offset between the cores.[19] Such an organization would readily be accommodated in a tilted rectangular phase. Nevertheless, we consider this latter possibility unlikely because a major reorganization of the mesogenic cores would be required to assemble the V=O groups into the observed polymeric crystal phase. The $D_{rd} \rightarrow K$ phase transitions for n = 12 and 14 are at ≈15–35 °C, and at these temperatures the samples are very viscous and it is unlikely that these materials are capable of such dramatic reorganizations. As a result, we favor a structure in which domains of weakly interacting V=O groups align unidirectionally within a column. This polar alignment may also be responsible for stabilizing the D_{rd} phase since a D_{rd} structure can accommodate an energetically favorable antiferroelectric arrangement, whereas the triangular symmetry of a hexagonal lattice leads to dipolar frustration.[13h,k]

Miscibility studies have been widely used to determine if liquid crystals exhibit the same phase. In discotic liquid crystals miscibility is very sensitive to mismatches in lattice constants, and miscibility studies must be performed on complexes that have the same length side chains. As expected, we find a lack of continuous miscibility between compounds displaying D_{rd} phases and those displaying D_{hd} phases. The M = Cu and M = Pd complexes which exhibit the same phases were totally miscible, and low melting mixtures can be easily prepared. We had considered it unlikely that the M = VO based D_{rd} phases would be miscible with the D_{rd} phases of the M = Cu and M = Pd complexes given their pyramidized shape and axial dipoles. However, we find complete miscibility of each family of D_{rd} compounds with a given side-chain length.

Complexes with 12 Side Chains. The greater side-chain density in series **4** produces a more varied and interesting phase behavior (Figure 5). Some of the rectangular phases were readily identified by their mosaic textures with prominent wedge shaped defects similar to plate 1 in Figure 2. The D_{rd} phases of **4** (n = 6, 8, M = Cu) also displayed very interesting feather textures (Figure 2, plate 8). This texture shows an unusual interwoven pattern of curved birefringent structures arranged such that the bright features intersect at 90° angles. The D_{hd} phases displayed typical natural textures with large regions of uniform extinction, fan patterns, and digitated leaf-shaped domains. We also observed the less common D_{hd} spine texture (Figure 2, plate 7) in the longer chain D_{hd} phases. In cases displaying multiple hexagonal phases,

(18) (a) Safinya, C. R.; Liang, K. S.; Varady, W. A.; Clark, N. A.; Anderson, G. *Phys. Rev. Lett.* **1984**, *53*, 1172. (b) Safinya, C. R.; Clark, N. A.; Liang, K. S.; Varady, W. A.; Chiang, L. Y. *Mol. Cryst. Liq. Cryst.* **1985**, *123*, 205.

(19) Piechocki, C.; Boulou, J.-C.; Simon, J. *Mol. Cryst. Liq. Cryst.* **1987**, *149*, 115.

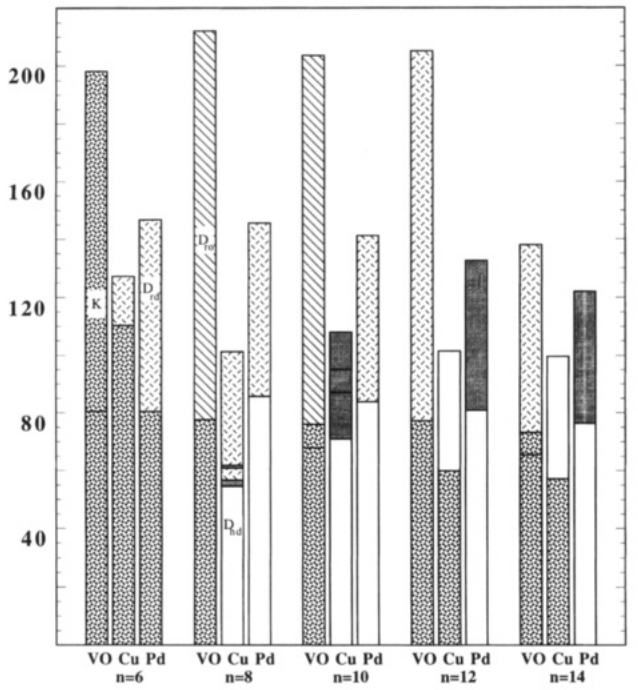

Figure 5. Bar graph showing the phase behavior of discotic compounds of series **4**. D_{ro} indicates a rectangular ordered columnar phase, and all other features are the same as indicated in Figure 1.

the fans or spines develop birefringent arcs similar to that observed shown in Figure 2, plates 2–4. The textures of D_{hd} phases of **4** (M = Cu, n = 8 and M = Pd, n = 8, 10) which were preceded by D_{rd} phases displayed fine needle patterns.

The M = Cu and M = Pd materials all display enantiotropic mesomorphism with low enthalpy clearing transitions and XRD patterns characteristic of D_{rd} and D_{hd} phases (Tables 3 and 4). The overall trends in phase behavior are similar to that observed for series **3** (Figure 5). Again we see a dominance of D_{rd} phases in the shorter side-chain analogues and a transition to D_{hd} phases with $n \geq 10$ for Cu and $n \geq 12$ for Pd. As discussed for series **3**, we attribute this behavior to a competition between attractive core–core interactions and dispersive forces. At intermediate side-chain lengths the balance between phases is nearly equal, and we see both D_{rd} and D_{hd} phases. For Cu (n = 8) and Pd (n = 8, 10) the D_{rd} phase appears first upon cooling the isotropic phase, and the D_{hd} phase is observed at lower temperatures. In this case, the transition to the D_{hd} phase at lower temperature cannot be the result of increased dispersive forces since these forces are generally diminished with decreasing temperature. One possible explanation is that the D_{hd} phase better accommodates preferred conformations of the alkyl side chains at low temperatures, since the more stable extended conformations will favor an arrangement of the cores normal to the column axis. The competition between the D_{rd} and D_{hd} phases appears to be particularly well balanced in the case of **4** (M = Cu, n = 8) which displays a very interesting and reproducible $D_{rd} \rightarrow D_{hd} \rightarrow D_{rd} \rightarrow D_{hd} \rightarrow D_{hd}$ phase sequence with cooling. The phase behavior is most clearly seen by XRD as shown in Figure 6, which shows the smooth transition between the phases. The M = Pd derivatives are more effective than the M = Cu analogues at suppressing the crystal phase, and all the M = Pd derivatives with C_8 or larger side chains were found to exhibit mesophases that could be cooled to room

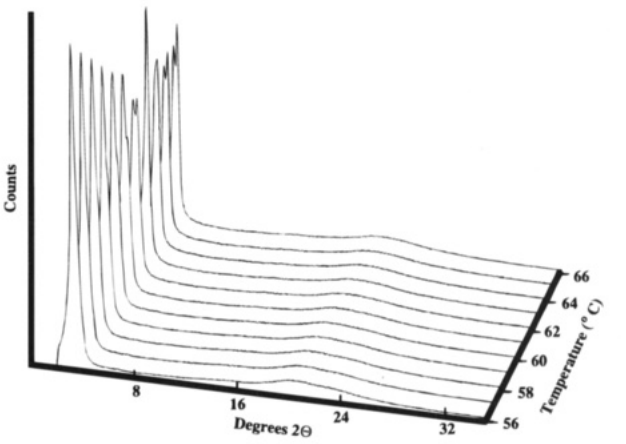

Figure 6. Three-dimensional plot of XRD data for **4** (M = Cu, n = 8) upon cooling. The merging and splitting of the low angle peaks illustrates an unusual $D_{rd} \rightarrow D_{hd} \rightarrow D_{rd} \rightarrow D_{hd}$ phase sequence.

temperature. As was the case for series **3**, the M = Pd analogues have higher clearing points than their Cu counterparts. These differences in clearing points appear to be greater in series **4** relative to series **3** indicating that the additional side chains facilitate greater intermolecular interactions.

The increased side-chain density has the most dramatic influences on the M = VO analogues. As can be seen from Figure 5, the isotropic phase transitions of all of the **4** M = VO analogues are 15–110 °C higher than those of the respective Cu and Pd homologues. Recall that for series **3** exactly the opposite is true with the M = VO analogues displaying lower clearing points than the analogueous M = Cu and M = Pd complexes. For **4** (M = VO, n = 6) some of the XRD peaks are not readily indexed to (hk0) or (00l) reflections (Table 4), hence this phase is clearly crystalline. Compounds **4** (M = VO, n = 8, 10) display an ordered phase which is identified as D_{ro} on the basis of XRD indexing (Table 4). This phase transforms to an isotropic state at higher temperatures (>50 °C) than the M = Cu and M = Pd materials. Similar to what has been previously observed in other D_{ro} materials, this phase is prone to large supercooling.[20] This feature in addition to other characteristics suggest to us that the D_{ro} phase exhibited by these materials is best characterized as a crystal phase. On the first heating XRD measurements show only the signals for the D_{ro} phase. However upon cooling from the isotropic phase, optical microscopy and XRD indicate that an isotropic phase is also present. Liquid-crystalline behavior is established when **4** (M = VO) is substituted with longer side chains (n = 12, 14), and these materials exhibit D_{rd} phases that are not prone to supercooling.

The dramatic differences between the M = VO compounds in series **3** and **4** suggest that the greater side-chain density enhances interactions between the metallomesogens. We find that samples of **4** (M = VO) are yellow and polymeric (V=O 888 cm^{-1}) when recrystallized from $CHCl_3$/EtOAc. It is interesting to note that recrystallization from THF/acetone produces green crystals (V=O 982 cm^{-1}). In the isotropic melt the materials are monomeric and exhibit a V=O stretching frequency of 1007 cm^{-1}, a value higher than observed for **3** (M =

(20) Barberá, J.; Esteruelas, M. A.; Levelut, A. M.; Oro, L. A.; Serrano, J. L.; Sola, E. *Inog. Chem.* **1992**, *31*, 732.

Table 3. Variable-Temperature XRD Data for the Liquid-Crystal Phases of Series 4

compound	mesophase	lattice constant (Å)	spacing (Å) obsd (calcd)	Miller indexes	compound	mesophase	lattice constant (Å)	spacing (Å) obsd (calcd)	Miller indexes
4, M = Cu					**4**, M = VO				
$n = 6$	D_{rd}, $P_{(2/a)}$ at 109 °C	$a = 48.82$	24.41 (24.41)	(200)	$n = 6^a$	crystal at 164 °C	$a = 46.48$	23.24 (23.24)	(200)
		$b = 22.72$	20.60 (20.60)	(110)			$b = 18.02$	16.80 (16.80)	(110)
			10.35 (10.30)	(220)				11.77 (11.75)	(310)
			9.08 (8.97)	(510)				9.01 (9.01)	(020)
			8.40 (8.32)	(420)				8.34 (8.40)	(220)
			7.53 (7.57)	(030)				7.15 (7.12)	(420)
$n = 8$	D_{rd} at 71 °C	$a = 49.86$	24.93	(200)				6.73	–
		$b = 25.77$	22.89	(110)				6.28 (6.23)	(710)
	D_{hd} at 63 °C	$a = 27.32$	23.66	(100)				5.91 (5.88)	(620)
	D_{rd} at 61 °C	$a = 46.92$	25.62	(110)				5.71	–
		$b = 30.58$	23.46	(200)				5.31	–
	D_{hd} at 56 °C	$a = 31.00$	26.85	(100)				5.05 (5.05)	(530)
	D_{hd} at 53 °C	$a = 31.30$	27.11	(100)	$n = 8^a$	D_{ro}, $C_{(2/m)}$ at 160 °C	$a = 51.40$	25.70 (25.70)	(200)
$n = 10$	D_{hd} at 98 °C	$a = 28.42$	24.61 (24.61)	(100)			$b = 19.98$	18.62 (18.62)	(110)
			14.35 (14.21)	(110)				13.09 (13.00)	(310)
	D_{hd} at 89 °C	$a = 28.66$	24.82 (24.82)	(100)				9.20 (9.14)	(510)
			14.46 (14.33)	(110)				7.91 (7.89)	(420)
	D_{hd} at 74 °C	$a = 29.04$	25.15 (25.15)	(100)				6.57 (6.60)	(130)
			14.64 (14.52)	(110)				6.22 (6.21)	(330)
	D_{hd} at 61 °C	$a = 32.09$	27.79	(100)				5.58 (5.59)	(530)
$n = 12$	D_{hd} at 74 °C	$a = 31.30$	27.11 (27.11)	(100)				4.8 (broad)	
			15.77 (15.65)	(110)				4.25	
$n = 14$	D_{hd} at 74 °C	$a = 37.95$	32.87 (32.87)	(100)	$n = 10^a$	D_{ro}, $C_{(2/m)}$ at 160 °C	$a = 54.80$	27.40 (27.40)	(200)
			18.73 (18.98)	(110)			$b = 22.42$	20.75 (20.75)	(110)
			16.43 (16.43)	(200)				14.25 (14.16)	(310)
4, M = Pd								10.39 (10.37)	(220)
$n = 6$	$D_{rd, C(2/m)}$ at 118 °C	$a = 46.48$	23.24 (23.24)	(200)				8.68 (8.68)	(420)
		$b = 19.29$	17.82 (17.82)	(110)				7.08 (7.08)	(620)
			12.16 (12.08)	(310)				6.17 (6.17)	(530)
			7.46 (7.42)	(420)				5.90 (5.85)	(820)
	$D_{rd, P(21/a)}$ at 54 °C	$a = 47.22$	23.61 (23.61)	(200)				4.75 (broad)	
		$b = 25.74$	22.60 (22.60)	(110)				4.30	
			13.52 (13.43)	(310)	$n = 12$	D_{rd}, $C_{(2/m)}$ at 160 °C	$a = 59.44$	29.72 (29.72)	(200)
			8.87 (8.87)	(510)			$b = 25.03$	23.07 (23.07)	(110)
			8.41 (8.44)	(130)				15.51 (15.53)	(310)
$n = 8$	$D_{rd, C(2/m)}$ at 118 °C	$a = 50.30$	25.15	(200)				11.53 (11.53)	(220)
		$b = 23.07$	20.97	(110)	$n = 14$	D_{rd}, $C_{(2/m)}$ at 110 °C	$a = 59.88$	29.94 (29.94)	(200)
	D_{hd} at 66 °C	$a = 30.08$	26.05 (26.05)	(100)			$b = 25.95$	23.81 (23.81)	(110)
			15.18 (15.04)	(110)				15.88 (15.82)	(310)
			12.89 (13.03)	(200)				12.98 (12.98)	(020)
$n = 10$	$D_{rd, C(2/m)}$ at 109 °C	$a = 55.86$	27.93 (27.93)	(200)				11.96 (11.91)	(220)
		$b = 27.25$	24.49 (24.49)	(110)					
			15.42 (15.37)	(310)					
			13.55 (13.62)	(020)					
	D_{hd} at 66 °C	$a = 34.32$	29.72 (29.72)	(100)					
			17.02 (17.16)	(110)					
$n = 12$	D_{hd} at 92 °C	$a = 32.91$	28.50 (28.50)	(100)					
			16.32 (16.45)	(110)					
	D_{hd} at 57 °C	$a = 37.08$	32.11 (32.11)	(100)					
			18.61 (18.54)	(110)					
$n = 14$	D_{hd} at 92 °C	$a = 33.95$	29.40 (29.40)	(100)					
			16.92 (16.97)	(110)					
			14.77 (14.70)	(200)					
	D_{hd} at 57 °C	$a = 38.87$	33.66	(100)					

[a] Data were taken on the first heating cycle to avoid coexistence of an isotropic phase (see text).

VO). In the D_{rd} phase of **4** (M = VO, $n = 12$, 14) the V=O band shifts to 982 cm^{-1}, and this behavior closely mirrors what was observed for the M = VO derivatives of series **3**. The 25 cm^{-1} shift of the V=O band to lower frequency is suggestive of weak dative associations. For the D_{ro} phase of **4** (M = VO, $n = 10$), the behavior is more complex, and at 170 °C a signal at 982 cm^{-1} and a broad signal at 999 cm^{-1} are observed. Cooling to 50 °C shifts the 999 cm^{-1} band to 991 cm^{-1}. This behavior indicates that the V=O groups are trapped in two different orientations which are a result of the coexistence of the D_{ro} and an isotropic phase.

Summary and Conclusions

This systematic investigation of 30 metal bis(β-diketonate) discotic complexes has revealed trends that provide a basis for consistent explanations of the observed behavior. These complexes have greater numbers of side chains than metal bis(β-diketonate)s studied previously and represent a major improvement in availability in liquid-crystalline compounds of this important class of compounds. We have found that nearly all of the compounds displayed well-behaved liquid crystallinity over a broad temperature range. While the structure property relationships of metallomesogens are complex and a comprehensive understanding is still elusive, our investigations have revealed some important lessons for the design of metallomesogens. Most notable is that increases in the side-chain density can enhance the ability of the metal center to influence the liquid crystalline behavior. Illustrative of this effect is the fact that the differences in the clearing

Table 4. DSC (10 °C/min) Data for Series 4 (Transition Temperatures (°C) and Enthalpies (in Parentheses, kcal/mol) for Heating and Cooling Cycles Given Above and Below the Arrows, Respectively)

Cu	$n = 6$	K	43.5 (2.96) / 40.0 (2.20)	K	110.3 (1.65) / 100.1 (1.83)	D_{rd}	127.2 (0.12) / 111.8 (0.24)	I						
	$n = 8$	D_{hd}	67.7 (8.55) / 54.6 (7.44)	D_{hd}	58.8 (0.05)	D_{rd}	62.8 (<0.01)	D_{hd}	63.8 (<0.01)	D_{rd}	103.3 (1.7) / 96.9 (1.6)	I		
	$n = 10$	D_{hd}	71 (0.07) / 67 (<0.01)	D_{hd}	87 (0.2) / 80.3 (0.38)	D_{hd}	95 (<0.01) / 94 (0.09)	D_{hd}	108.0 (1.9) / 102.7 (1.75)	I				
	$n = 12$	K	59.9 (9.66) / 51.7 (9.44)	D_{hd}	101.5 (1.42) / 93.8 (1.55)	I								
	$n = 14$	K	44.0 (6.11) / 37.9 (7.02)	K	57.2 (8.18) / 48.9 (8.74)	D_{hd}	99.6 (2.10) / 94.9 (2.29)	I						
Pd	$n = 6$	K	80.4 (9.82) / 63.0 (9.42)	D_{rd}	146.7 (3.46) / 142.6 (3.35)	I								
	$n = 8$	D_{hd}	85.7 (9.66) / 75.2 (9.69)	D_{rd}	145.5 (2.49) / 140.3 (2.16)	I								
	$n = 10$	D_{hd}	83.8 (11.3) / 75.6 (11.3)	D_{rd}	141.2 (3.32) / 137.0 (3.03)	I								
	$n = 12$	D_{hd}	80.8 (11.5) / 73.9 (11.3)	D_{hd}	132.6 (2.53) / 127.9 (2.43)	I								
	$n = 14$	D_{hd}	76.4 (9.83) / 69.5 (10.7)	D_{hd}	122.0 (1.98) / 116.9 (1.78)	I								
VO	$n = 6$	K	80.4 (7.80) / 62.4 (8.29)	K	198.1 (7.83) / 190.4 (6.24)	I								
	$n = 8$	K	77.6 (10.7) / 66.2 (10.3)	D_{ro}	212.1 (3.90)[a] / 210.1 (4.05)[a]	I								
	$n = 10$	K	68.0 (4.60) / 59.1 (4.88)	K	76.1 (6.26) / 68.5 (6.25)	D_{ro}	203.6 (1.94)[a] / 197.1 (1.91)[a]	I						
	$n = 12$	K	77.2 (26.1) / 71.4 (25.2)	D_{rd}	205.2 (6.45) / 200.4 (7.88)	I								
	$n = 14$	K	65.5 (47.9) / 59.4 (30)	K	73.3 (10.8) / 63.6 (30)	D_{rd}	138.0 (5.10) / 132.0 (5.02)	I						

[a] XRD and optical studies indicate that only part of the sample transforms to the D_{ro} phase.

points of the M = Cu and M = Pd analogues are greater in the 12 side-chain series than the 10 side-chain series. In addition, unusually large differences are observed between the 10 and 12 side-chain analogues of the M = VO complexes. Consistent with this greater organization, we find that the ability of the M = VO complexes to form linear chains in M = VO complexes is enhanced by the added side chains in **3** and **4** since no other vanadyl bis(β-diketonate)s have been reported to display these polymeric structures. This behavior is indicative of greater core−core interactions, and such features are important for the formation of new metallomesogen-based materials with extended electronic and magnetic interactions. We believe that this effect is principally entropic in nature and that the greater density of side chains enhances the organization of the cores relative to each other. In future investigations we plan to test the applicability of increased side-chain density to realize novel properties from metallomesogenic materials.

Experimental Section

General Methods. The methyl benzoate ester derivatives and the acetophenone derivatives were synthesized by using literature procedures.[7c,h] Unless otherwise noted, all chemicals and solvents were reagent grade and used without further purification. Dimethoxyethane (DME) was dried over sodium benzophenone ketyl. ^1H and ^{13}C NMR spectra were measured on a Bruker AC-250. Multiplicities are indicated as s (singlet), d (doublet), t (triplet), m (multiplet). Infrared spectra were recorded on a Perkin-Elmer 1760-X FTIR using polystyrene as a standard. Room-temperature IR measurements were performed using Nujol mull methods, while the variable temperature studies were performed by sandwiching a thin film of sample between two KBr plates in a Mettler FP82 hot stage in which the glass heat shields had been removed. FAB mass spectroscopy was performed on a VG analytical ZAB-E instrument using CH_2Cl_2 as a solvent and 3-nitrobenzyl alcohol as the matrix. Elemental analyses for carbon, hydrogen, and nitrogen were performed on a Perkin-Elmer 240C elemental analyzer, and analysis results are given in Table 5. DSC investigations were carried out on a Perkin-Elmer DSC-7. Optical microscopy was carried out on a Leica polarizing microscope in combination with a Mettler FP 80HT/FP 82HT hot stage. X-ray diffraction studies were carried out on samples in capillary tubes with an INEL diffractometer with a 2 kW Cu Kα X-ray source fitted with an INEL CPS-120 position sensitive detector and a home-built oven. The temperature was controlled by a Minco CT 137 temperature controller. The detector was calibrated using mica and silicon standards which were obtained from the National Bureau of Standards (NBS).

1-(3′,4′-Dihexyloxyphenyl)-3-(3,4″,5″-trihexyloxyphenyl)-propane-1,3-dione (General Procedure for Diketonate Ligands). The procedure given by Ohta[7c] was adapted to make the title compound. A mixture of 8.17 g (18.7 mmol) of methyl 3,4,5-trihexyloxybenzoate and 6.00 g (18.7 mmol) of 3,4-dihexyloxyacetonephenone was dissolved in dry dimethox-

Table 5. Elemental Analysis of all Cu, Pd, and VO Bis(β-diketone) Complexes[a]

	% carbon		% hydrogen	
complex	calcd	found	calcd	found
3, Cu				
$n = 6$	69.90	68.44	9.57	9.51
$n = 8$	73.80	73.22	10.13	10.13
$n = 10$	75.41	75.96	10.71	11.24
$n = 12$	76.63	76.72	11.15	11.84
$n = 14$	77.59 (76.55)[b]	75.91	11.48 (11.47)[b]	11.14
3, Pd				
$n = 6$	69.54	70.15	9.21	9.81
$n = 8$	72.05	71.99	9.93	10.64
$n = 10$	73.87	74.73	10.50	11.23
$n = 12$	75.25	74.85	10.94	11.26
$n = 14$	76.35	76.97	11.29	11.28
3, VO				
$n = 6$	71.40	70.76	9.38	9.48
$n = 8$	73.64	73.79	10.14	10.51
$n = 10$	75.28	75.67	10.69	11.31
$n = 12$	76.51	75.69	11.13	11.33
$n = 14$	77.49	77.91	11.47	11.85
4, Cu				
$n = 6$	70.14	68.42	9.85	9.92
$n = 8$	73.89	72.66	10.53	10.70
$n = 10$	75.53	74.10	11.07	11.20
$n = 12$	76.78	74.90	11.48	11.56
$n = 14$	77.76 (76.92)[b]	75.87	11.80 (11.71)[b]	11.83
4, Pd				
$n = 6$	69.81	70.11	9.53	10.03
$n = 8$	72.42	72.03	10.24	10.39
$n = 10$	74.26	74.40	10.80	11.41
$n = 12$	75.66	76.12	11.22	11.73
$n = 14$	76.75	76.50	11.55	12.01
$n = 16$	77.63	77.54	11.82	12.46
4, VO				
$n = 6$	71.47	69.98	9.69	9.43
$n = 8$	73.75 (70.27)[c]	71.07	10.51 (9.91)[c]	10.72
$n = 10$	75.43	75.36	11.06	11.64
$n = 12$	76.69 (73.93)[c]	74.45	11.46 (10.94)[c]	11.15
$n = 14$	77.74	75.95	11.70	11.71

[a] TGA (room temperature to 140 °C) showed minor weight loses (0.2–1.24%) for samples with disagreements in calculated and experimental elemental compositions indicating small amounts of entrapped solvent. [b] Calculated to include 2 mol of H_2O. [c] Calculated to include 1 mol of $CHCl_3$.

yethane (DME) and was refluxed for 3 h in the presence of 2.70 g of 90% sodium hydride (101.2 mmol). The resulting brown-yellow solution was cooled and poured into ice/water/HCl(aq), where the excess NaH was quenched and the diketone was neutralized. The product was extracted with two 80 mL portions of diethyl ether and washed with distilled water three times. After the ether solution was dried with $MgSO_4$, it was evaporated to give a deep brown oily liquid which was purified by silica chromatography with hexane/diethyl ether (10:1) as an eluent to give the diketone product (12.2 g, 90% yield) as a highly viscous brown liquid. ^{1}H NMR ($CDCl_3$) 0.86–0.92 (m, $O(CH_2)_5\mathbf{CH_3}$), 1.30–1.47 (m, $OCH_2CH_2\mathbf{(CH_2)_3}CH_3$), 1.69–1.86 (m, $OCH_2\mathbf{(CH_2)_3}CH_2CH_3$), 3.97–4.08 (m, $\mathbf{OCH_2}(CH_2)_4CH_3$), 4.49 (s, $CO\mathbf{CH_2}CO$), 6.67 (s, COCHCOH), 6.87, 6.90 (d, **ArH**), 7.16 (s, **ArH**), 7.53, 7.56 (s + d, **ArH**), 17.13 (s, COCHCO**H**). ^{13}C NMR ($CDCl_3$) 14.0, 22.6, 25.6, 25.7, 29.0, 29.1, 29.3, 30.2, 31.5, 31.7, 69.0, 69.4, 73.5, 92.1, 105.9, 112.1, 112.2, 121.2, 128.1, 130.5, 148.91, 153.1, 184.2, 185.4. MS *m/e* 725 ($M + H^+$). Elemental Anal. Calcd: C 74.60, H 9.94. Found: C 75.45, H 10.33.

1,3-Bis(3′,4′,5′-trihexyloxyphenyl)-1,3-propanedione. This compound was synthesized by the same procedure as described for 1-(3′,4′-dibutyloxyphenyl)-3-(3″,4″,5″-tributyloxyphenyl)propane-1,3-dione with 85% yield. ^{1}H NMR ($CDCl_3$) 0.84–0.90 (m, $OCH_2(CH_2)_4\mathbf{CH_3}$), 1.29–1.46 (m, $OCH_2CH_2\mathbf{(CH_2)_3}CH_3$), 1.67–1.85 (m, $OCH_2\mathbf{CH_2}(CH_2)_3CH_3$), 3.95–4.05 (m, $\mathbf{OCH_2}(CH_2)_4CH_3$), 4.47 (s, $CO\mathbf{CH_2}CO$), 6.60 (s, COCHCOH), 7.14 (s, **ArH**), 17.03 (s, OCCHCO**H**). ^{13}C NMR ($CDCl_3$) 14.0, 22.6, 22.6, 25.7, 29.3, 30.3, 31.6, 31.7, 69.6, 73.6, 92.7, 106.3, 130.5, 142.5, 153.1, 185.2. MS *m/e* 826 ($M + H^+$). Elemental Anal. Calcd: C 74.34, H 10.23. Found: C 75.69, H 10.60.

Bis[1-(3′,4′-didecenoxyphenyl)-3-(3″,4″,5″-tridecenoxyphenyl)propane-1,3-dionato]copper(II) (General Procedure for 3, M = Cu). A mixture of 2.0 g (1.99 mmol) of diketone ligand, 0.32 g (1.6 mmol) of hydrated copper acetate, and 20 mL of 95% ethanol was stirred and refluxed for 2 h. Green solids precipitated when the reaction was cooled. The product was filtered, washed with methanol and recrystallized from THF/MeOH to give 1.85 g (90% yield) of green solid. IR (thin film) 1600 (C=C), 1541 (C=O), 1194 (C–H in-plane bending), 776 (C–H out-of-plane bending) cm^{-1}. UV/vis (hexane) λ_{max} (log ϵ) 208 (4.92), 324 (4.57), 366 (4.81). MS *m/e* 2070 ($M + H^+$). Elemental Anal. Calcd: C 75.41, H 10.71. Found: C 75.96, H 11.24.

Bis[1,3-bis(3′,4′,5′-trioctyloxyphenyl)-1,3-propanedionato]copper(II) (General Procedure for 4, M = Cu). This complex was made using the same way as for bis[1-(3′,4′-didecenoxyphenyl)-3-(3″,4″,5″-tridecenoxyphenyl)propane-1,3-dionato]copper(II) with 90% yield. IR (thin film) 1587 (C=C), 1543 (C=O), 1192 (C–H in-plane bending), 780 (C–H out-of-plane bending) cm^{-1}. MS *m/e* 2049 ($M + H^+$). Elemental Anal. Calcd: C 73.89, H 10.53. Found: C 72.66, H 10.70.

Bis[1-(3′,4′-dihexyloxyphenyl)-3-(3″,4″,5″-trihexyloxyphenyl)propane-1,3-dionato]palladium(II) (General Procedure for 3, M = Pd). The procedure given by Rao[8d] was adapted to make the title compound. A stirred mixture of 1.0 g (1.38 mmol) of diketone ligand, 0.19 g (1.38 mmol) of K_2CO_3, 0.25 g (1.10 mmol) of palladium acetate, and 10 mL of acetonitrile was heated to 70 °C. $CHCl_3$ was added until the suspension turned to clear brown. The reaction was cooled after 16 h, and $CHCl_3$ was added to dissolve the palladium complex. The deep brown solution was filtered by aid of Celite 545. Removal of solvent resulted in yellow powder which was recrystallized with CH_2Cl_2/CH_3CN to give 0.86 g (80% yield) of yellow product. ^{1}H NMR ($CDCl_3$) 0.87–0.91 (m, $O(CH_2)_5\mathbf{CH_3}$), 1.32–1.55 (m, $OCH_2CH_2\mathbf{(CH_2)_3}CH_3$), 1.68–1.86 (m, $OCH_2\mathbf{CH_2}(CH_2)_3CH_3$), 3.98–4.05 (m, $\mathbf{OCH_2}(CH_2)_4CH_3$), 6.55 (s, COCHCO), 6.82, 6.85 (6.83, 6.86 as for the tautomer) (d, **ArH**), 7.12 (7.10 as for the tautomer) (s, **ArH**), 7.47–7.55 (m, **ArH**). ^{13}C NMR ($CDCl_3$) 14.0, 22.6, 25.7, 25.7, 25.8, 29.1, 29.4, 30.3, 31.6, 31.6, 31.7, 69.0, 69.4, 69.6, 73.5, 95.2, 106.7, 112.1, 113.5, 121.4, 129.3, 132.1, 141.5, 148.6, 152.5, 152.7, 180.8, 180.8. UV/vis (hexane) λ_{max} (log ϵ) 214 (4.91), 330 (4.66), 382 (4.54), 408 (4.30). MS *m/e* 1554 ($M + H^+$). Elemental Anal. Calcd: C 69.54, H 9.21. Found: 70.15, H 9.81.

Bis[1,3-bis(3′,4′,5′-trihexyloxyphenyl)-1,3-propanedionato]palladium(II) (General Procedure for 4, M = Pd). This complex was made by using the same procedure as for bis[1-(3′,4′-dihexyloxyphenyl)-3-(3″,4″,5″-trihexyloxyphenyl)-propane-1,3-dionato]palladium(II) with 75% yield. ^{1}H NMR ($CDCl_3$) 0.85–0.91 (m, $O(CH_2)_5\mathbf{CH_3}$), 1.30–1.48 (m, $OCH_2CH_2\mathbf{(CH_2)_3}CH_3$), 1.68–1.83 (m, $OCH_2\mathbf{CH_2}(CH_2)_3CH_3$), 3.97–4.02 (m, $\mathbf{OCH_2}(CH_2)_4CH_3$), 6.49 (s, COCHCO), 7.09 (s, **ArH**). ^{13}C NMR ($CDCl_3$) 14.0, 22.6, 22.6, 25.7, 25.8, 29.4, 30.3, 31.6, 31.7, 69.4, 73.6, 96.0, 106.8, 131.9, 141.7, 152.8, 181.4. MS *m/e* 1754 ($M + H^+$). Elemental Anal. Calcd: C 69.81, H 9.53. Found: C 70.11 H 10.03.

Bis[1-(3′,4′-didodecenoxyphenyl)-3-(3″,4″,5″-tridodecenoxyphenyl)propane-1,3-dionato]oxovanadium-(IV) (General Procedure for 3, M = VO). The literature procedure[7i,j] was adapted to make this compound. All the solvents were degassed before using and the reaction as well as recrystallization was protected by nitrogen gas. To 10 mL of 95% ethanol was added 1.0 g (0.87 mmol) of diketone ligand. The suspension was heated until the ligand dissolved. To the stirred ligand solution was added dropwise 2 mL of 0.12 g (0.63 mmol) of vanadyl sulfate aqueous solution. The reaction solution turned to green immediately, and some green oily products began to precipitate. At this point a 1 mL aqueous solution of 0.059 g (0.43 mmol) of potassium carbonate was added dropwise to neutralize the solution and drive the reaction completion. The reaction was then heated to 80 °C for 3 h and was then cooled to room temperature. The product was extracted by two portions of 20 mL of methylene chloride and washed twice with distilled water. Removal of CH_2Cl_2 resulted in yellow solid which was recrystallized with chloro-

form/ethyl acetate to give 0.72 g (70% yield) of a yellow product with V=O stretching frequency at 898 cm^{-1}. Recrystallization with tetrahydrofuran and acetone gave a green product with a V=O stretching frequency at 985 cm^{-1}. IR of yellow form (Nujol mull) 1604 (C=C), 1543 (C=O), 1199 (C−H in-plane bending), 898 (V=O), 776 (C−H out-of-plane bending) cm^{-1}. IR of green form (Nujol mull) 1595 (C=C), 1541 (C=O), 1193 (C−H in-plane bending), 985 (V=O), 793 (C−H out-of-plane bending) cm^{-1}. UV/vis (hexane) λ_{max} (log ϵ) 212 (4.90), 378 (4.83). MS *m/e* 2354 ($M + H^+$). Elemental Anal. Calcd: C 76.51, H 11.13. Found: C 75.69, H 11.33.

Bis[1,3-di(3′,4′,5′-tridecenoxyphenyl)-1,3-propanedionato]oxovanadium(IV) (General Procedure for 4, M = VO). This compound was synthesized by using the same procedure as for bis[1-(3′,4′-didodecenoxyphenyl)-3-(3″,4″,5″-tridodecenoxyphenyl)propane-1,3-dionato] oxovanadium(IV) with 65% yield. Recrystallization from chloroform and ethyl acetate yielded a yellow powder with a V=O stretching frequency at 888 cm^{-1}, while recrystallization from tetrahydrofuran and acetone gave a green product with a V=O stretching frequency at 982 cm^{-1}. IR of the yellow form (Nujol mull) 1591 (C=C), 1532 (C=O), 1195 (C−H in-plane bending), 888 (V=O), 783 (C−H out-of-plane bending) cm^{-1}. IR of the green form (Nujol mull) 1587 (C=C), 1546 (C=O), 982 (V=O) cm^{-1}. MS *m/e* 2387 ($M + H^+$). Elemental Anal. Calcd: C 75.43, H 11.06. Found: C 75.36, H 11.64.

Acknowledgment. We thank the Office of Naval Research and NSF (DMR-9258298 and DMR-9503572) for financial support of this work.

Supporting Information Available: Infrared spectra corresponding to the data reported in the experimental section (6 pages). This material is contained in many libraries on microfiche, immediately following this article in the microfilm version of the journal, can be ordered from the ACS, and can be downloaded from the Internet; see any current masthead page for ordering information.

CM9502840